Biochimica et Biophysica Acta 1807 (2011) 451–457

Contents lists available at ScienceDirect

Biochimica et Biophysica Acta

journal homepage: www.elsevier.com/locate/bbabio

# Electron transfer to the active site of the bacterial nitric oxide reductase is controlled by ligand binding to heme $b_3$

Sarah J. Field [a], M. Dolores Roldan [b], Sophie J. Marritt [a], Julea N. Butt [a], David J. Richardson [a], Nicholas J. Watmough [a,*]

[a] Centre for Molecular and Structural Biochemistry, School of Biological Sciences and School of Chemistry, University of East Anglia, Norwich Research Park, Norwich NR4 7TJ, UK
[b] Departamento de Bioquímica y Biología Molecular, Edificio Severo Ochoa, 1ª planta. Campus Universitario de Rabanales, Universidad de Córdoba. 14071-Córdoba, Spain

ARTICLE INFO

*Article history:*
Received 11 October 2010
Received in revised form 26 January 2011
Accepted 30 January 2011
Available online 4 February 2011

*Keywords:*
Carbon monoxide
Denitrification
Electron transfer
Hemes
Nitric oxide

ABSTRACT

The active site of the bacterial nitric oxide reductase from *Paracoccus denitrificans* contains a dinuclear centre comprising heme $b_3$ and non heme iron ($Fe_B$). These metal centres are shown to be at isopotential with midpoint reduction potentials of $E_m \approx +80$ mV. The midpoint reduction potentials of the other two metal centres in the enzyme, heme *c* and heme *b*, are greater than the dinuclear centre suggesting that they act as an electron receiving/storage module. Reduction of the low-spin heme *b* causes structural changes at the dinuclear centre which allow access to substrate molecules. In the presence of the substrate analogue, CO, the midpoint reduction potential of heme $b_3$ is raised to a region similar to that of heme *c* and heme *b*. This leads us to suggest that reduction of the electron transfer hemes leads to an opening of the active site which allows substrate to bind and in turn raises the reduction potential of the active site such that electrons are only delivered to the active site following substrate binding.



## 1. Introduction

The respiratory nitric oxide reductases (NORs) are integral membrane proteins found in bacteria that catalyse the reductive condensation of two molecules of nitric oxide (NO) to form nitrous oxide ($N_2O$) [1,2]:

$$2NO + 2H^+ + 2e^- \rightarrow N_2O + H_2O$$

This reaction is the third step in the process of bacterial denitrification in which the soluble anions nitrate ($NO_3^-$) and nitrite ($NO_2^-$) are converted enzymatically to nitrous oxide [3].

$$NO_3^- \rightarrow NO_2^- \rightarrow \text{nitric oxide(NO)} \rightarrow N_2O \rightarrow N_2$$

A fourth enzyme, nitrous oxide reductase, further reduces $N_2O$ to dinitrogen which is released to the atmosphere. However, when nitrous oxide reductase is absent or inactive the major product of denitrification is $N_2O$, a significant greenhouse gas [4]. In recent decades, the largest source of anthropogenic $N_2O$ emissions has been agricultural soils, in part due to the increased use of artificial fertilisers containing nitrates. Consequently there is a considerable interest in enzymes, including the bacterial NOR, that are responsible for the production and/or consumption of $N_2O$.

Three types of respiratory NORs have been described in Eubacteria [2], and the X-ray structure of the cytochrome *c* dependent NOR (cNOR) from *Pseudomonas aeruginosa* which is purified as a two-subunit complex, NorBC, has been recently reported [5]. This will help to interpret the detailed biochemical and spectroscopic information that has been obtained on the NorBC from *Paracoccus denitrificans* [1]. NorC is a mono-heme *c*-type cytochrome that possesses an N-terminal transmembrane helix that anchors the heme domain to the periplasmic face of the cytoplasmic membrane and relays electrons from the periplasmic donor proteins (cytochromes and cupredoxins) to the catalytic subunit, NorB [5,6]. While functionally distinct, NorB is structurally related to the catalytic subunit (subunit I) of the respiratory heme–copper oxidases (HCuOs), e.g. cytochrome $aa_3$ oxidase [5,7]. NorB contains three metal centres, a magnetically isolated heme known as heme *b*, a second heme, known as heme $b_3$, and a non heme iron ($Fe_B$) which is coordinated by three histidine residues that are conserved in all typical HCuOs and a glutamate residue that is conserved in all NORs [5]. Heme $b_3$ and $Fe_B$ form a dinuclear centre at the active site of the enzyme and are close enough to be magnetically coupled [8].

In the fully oxidised enzyme as isolated from *P. denitrificans* the two components of the dinuclear centre are linked by a μ-oxo bridge and heme $b_3$ lacks a proximal ligand [9]. Upon partial reduction the μ-oxo bridge is broken and opens up the active site to binding of small molecules e.g. $CN^-$ ions [10]. This change is reported by a shift in the position of a ligand to metal charge transfer (CT) band associated with ferric heme $b_3$ in the UV–visible spectrum of NOR from 595 nm

* Corresponding author at: School of Biological Sciences, University of East Anglia, Norwich, NR4 7TJ, UK. Tel.: +44 1603 592179; fax: +44 1603 592250.
*E-mail address:* n.watmough@uea.ac.uk (N.J. Watmough).

0005-2728/$ – see front matter © 2011 Elsevier B.V. All rights reserved.
doi:10.1016/j.bbabio.2011.01.009

(oxidised active site with a μ-oxo bridge) to either 605 nm or 630 nm [10–12]. The shift is pH dependent and consistent with binding of histidine as the proximal ligand to high-spin ferric heme $b_3$ species with distal ligation by $OH^-$ (605 nm) at pH 8.5 or $H_2O$ (630 nm) at pH 6.0 [11].

Mediated redox titrations of NorBC monitored using UV/vis spectroscopy were used to assign reduction potentials to the four metal centres of the enzyme at pH 7.6 [10]. Analysis of the absorbance changes seen at 550 nm and 560 nm in response to changes in the solution potential allowed the midpoint reduction potentials for the low spin hemes *c* (+310 mV) and *b* (+345 mV) to be measured [11]. These hemes are predicted to accept electrons from periplasmic donors, such as cytochrome $c_{550}$ ($E_m = +256$ mV) or pseudoazurin ($E_m = +230$ mV) and their recorded midpoint reduction potentials are consistent with a role in facilitating rapid electron transfer.

The changes in absorbance due to the reduction of hemes *b* and *c* are accompanied by changes in the near infrared region (590–640 nm) that reflect changes at the dinuclear centre. Hence the reduction of NorBC can also be monitored by the decrease in absorbance at 595 nm which is described by a two phase curve. At pH 7.6 partially reduced NorBC contains a mixed population of His/$OH^-$ and His/$H_2O$ ligated ferric heme $b_3$. This means that the initial decrease of absorbance observed at 595 nm is accompanied by an increase in the 605 nm and 630 nm features [11]. Further reduction of NorBC results in the complete loss of these CT bands such that the second, lower potential, phase of the redox titration monitored at 595 nm reports the midpoint reduction potential of heme $b_3$ (+60 mV) [11].

The first, higher potential, phase of the titration monitored at 595 nm was interpreted in terms of reporting the reduction of the non heme $Fe_B$ which causes the μ-oxo bridge to break and the active site to open. This part of the curve was used to determine a midpoint reduction potential for the $Fe_B$ centre (+230 mV), an analysis that led to the suggestion the enzyme was active in a three electron reduced state. However a major constraint on this interpretation is that the properties of the non heme $Fe_B$ were inferred from spectroscopic shifts due to ligation changes at heme $b_3$ rather than any change in the oxidation state of the non heme $Fe_B$ itself. This was necessary because the $Fe_B$ centre in NOR is spectroscopically silent. Weak signals that arise from non heme $Fe_B$ in the visible spectrum of NorBC are masked by the intense signals of the hemes and the characteristic signal in the EPR spectrum of a ferric mono-nuclear non-heme iron centre at $g' = 4.3$ is rendered silent due to coupling to the heme $b_3$ [8]. In the present work we present a method to spectroscopically isolate and probe the nature of the $Fe_B$ site, which allows a re-appraisal of earlier spectro-potentiometic studies.

## 2. Materials and methods

### 2.1. Cell growth and purification

NorBC used in this study was purified from *P. denitrificans* strain 93.11 (Δ*cta*DI, Δ*cta*CII, *qox*B::*kan*$^R$) grown in a Bioengineering 100-litre fermenter or 8×5-litre Duran flasks in minimal medium under anaerobic denitrifying conditions. The enzyme was purified as described by Field et al. [13].

### 2.2. Spectroscopy

Electronic absorption spectra were recorded on a Varian Cary 50 BIO, an Aminco DW2000 or a JASCO V-500 UV–visible spectrophotometer. The concentration of NorBC was calculated using an extinction coefficient $\varepsilon_{411} = 3.11 \times 10^5\ M^{-1}\ cm^{-1}$ [12].

EPR spectra were recorded on either a Bruker ELEXSYS 500 spectrometer with an ER049X SuperX microwave bridge and an SHQ cavity or on an X-band ER200-D spectrometer (Bruker Spectrospin) interfaced to an ESP1600 computer. Low temperature experiments were performed using an Oxford Instruments ESR-900 helium cryostat and ITC3 temperature controller.

### 2.3. Electrodic poising of NorBC for EPR spectroscopy

All manipulations were carried out in an anaerobic glove box (Belle Technology) under a $N_2$ atmosphere and at 4 °C. Samples of NorBC at a concentration of 135 μM in 20 mM BTP, 50 mM NaCl, 0.02% (wt./vol.) dodecyl-β-D-maltoside (DDM) adjusted to either pH 6.0 or pH 8.5 as desired were supplemented with the following redox mediators at a final concentration of 10 μM; Dichlorophenol (+217 mV), trimethylhydroquinone (+100 mV), phenazine methyl sulphate (+80 mV), 5-hydroxynapthoquinone (+45 mV), duroquinol (0 mV), menadione (−80 mV), 9,10-anthraquinone-2,6-disulfonic acid (−185 mV), safranine (−289 mV), and benzyl viologen (−350 mV). Samples were poised at a defined potential using a three-electrode cell configuration incorporating an $Al_2O_3$ polished carbon 'pot' working electrode. The reference electrode was calomel in saturated KCl, (SCE) and this contacted the sample via a Luggin tip. The counter electrode was a Pt-wire physically separated from the sample by a Vycor frit. The potential was controlled and the resulting flow of current measured by a PGSTAT 12 potentiostat (Autolab) controlled by GPES software. Samples were stirred during poising and equilibrium was judged to have been reached when the monitored current fell to zero. Equilibrated samples were transferred to EPR tubes in the glove box, the tubes were sealed and the samples frozen in liquid nitrogen within 1 minute. Experimental potentials were referenced to the SHE by the addition of 241 mV.

### 2.4. Preparations of partially reduced forms of NorBC in a CO environment

Chemical titrations under an atmosphere of CO were carried out in an anaerobic glove box (Belle Technology) under a $N_2$ atmosphere using $EuCl_2$:EGTA as the reductant [14]. Titrations were monitored with a voltmeter at 4 °C in a water jacketed glass cell fitted with ports for an SCE, a platinum wire counter electrode, a glass bulb filled with CO and a needle to allow the injection of reductant. NorBC samples in the concentration range 50–60 μM were buffered in 20 mM BTP, 50 mM NaCl, 0.02% (wt./vol.) DDM pH 6.0 and supplemented with the mediator cocktail described in Section 2.3. Once the required potential was reached samples were transferred to EPR tubes in the glove box, the tubes were sealed and the samples frozen in liquid nitrogen within 1 minute.

### 2.5. Spectroelectrochemical titrations of NorBC

Reductive titrations of NorBC using sodium dithionite were carried out at 20 °C essentially as described by Dutton [15]. Samples of NorBC (5–20 μM) were prepared in 20 mM Bis–Tris–propane (BTP), 340 mM NaCl, 0.02% (wt./vol.) DDM, adjusted to a known pH in the range 6.0–8.5 supplemented with the following cocktail of redox mediators at a final concentrations of 20 μM: Diaminodurene (+240 mV), phenazine methyl sulphate (+80 mV), phenazine ethyl sulphate (PES) (+55 mV), 5-hydroxynapthoquinone (+45 mV), 6-anthraquinone-2,6-disulfonic acid (−184 mV), 5-anthraquinone-2-sulfonic acid (−230 mV) and benzyl viologen (−350 mV). Quinhydrone ($E_{m,pH\ 7.0} = +295$ mV) was used as a redox standard.

### 2.6. Electrodic titrations of NorBC under a CO atmosphere

These experiments were performed in a 10 mm path length cuvette which accommodated a platinum foil working electrode, gas inlet and CO bulb attachment. The counter electrode was a platinum wire separated from the sample by a Vycor frit. An Ag/AgCl reference electrode was connected via a luggin tip. Samples of NorBC (20 μM) were prepared in 20 mM BTP, 100 mM NaCl, 0.02% (wt./vol.) DDM, pH 6.0. Redox mediators were included in the sample at final concentrations of 40 μM

as follows; ferrocene acetic acid (+365 mV), diaminodurene (+240 mV), ruthenium hexamine chloride (+200 mV), trimethylhydroquinone (+100 mV), 5-hydroxynapthoquinone (+45 mV), duroquinol (0 mV), menadione (−80 mV), 9,10-anthraquinone-2,6-disulfonic acid (−185 mV), and 5-anthraquinone-2-sulfonic acid (−230 mV). The spectroelectrochemical cell containing the sample was sparged with nitrogen gas then with CO gas and a bulb containing CO gas was attached to the cell in order to maintain a constant atmosphere of CO during the experiment. The desired potential was applied to the cell using a PGSTAT 12 potentiostat controlled by GPES software (Autolab). The samples were stirred and equilibrium was judged to have been reached when the monitored current fell to zero. Recorded potentials were referenced to the SHE by the addition of 197 mV.

## 3. Results and discussion

### 3.1. Potential dependent changes in the X-band EPR spectrum of NorBC

To investigate the redox properties of the non-heme Fe centre of NorBC, continuous wave X-band EPR spectra were collected from samples poised electrodically at a range of potentials. At pH 6 the EPR spectrum of the as prepared fully oxidised NorBC is as previously described [12] (Fig. 1). Two features typical of low spin, S = 1/2, hemes are visible in the spectrum, the rhombic trio ($g_x$, $g_y$, and $g_z$, = 3.00, 2.25 and 1.46), and high $g_{max}$ species, $g_z$ = 3.55, have previously been assigned to the low spin heme *b* and heme *c* respectively [12]. The signal seen at $g$ = 2.01 has previously been attributed to a trace of a contaminating [3Fe-4S] cluster [12]. The heme $b_3$ and non heme $Fe_B$ in the active site of NorBC have been shown to be anti-ferromagnetically coupled, leading to the absence of EPR signals from these metal centres [8]. Peaks seen in the $g$ = 6 and $g$ = 4.3 regions of the pH 6.0 spectrum where signals from these centres are expected to arise are thought to be due to small populations of protein (<5%) where the dinuclear centre is uncoupled [8]. After reducing the sample to +100 mV, EPR signals due to the low spin hemes *b* and *c* disappeared, consistent with these being high-potential centres [11]. The residual signal at $g$ = 3.01 is of a slightly different line shape to that seen in the oxidised spectrum and has previously been attributed to a small amount of uncoupled low spin heme $b_3$ in the partially reduced NorBC [13].

The spectra of NorBC samples poised at potentials below +100 mV showed little change of the signals in the $g$ = 6 and $g'$ = 4.3 regions, where heme $b_3$ and non-heme iron, respectively, are expected to be detected (Fig. 1). This is significant because if the $Fe_B$ has a midpoint reduction potential close to those of the low spin heme *b* and heme *c*, as inferred from previous UV–visible potentiometric titrations [11,12], then as the titration proceeds the signal at $g$ = 6, from the heme $b_3$, should become increasingly intense as the ferric $Fe_B$ becomes reduced and the coupling between heme $b_3$ and $Fe_B$ is broken. That this does not happen suggests that the midpoint reduction potentials of heme $b_3$ and $Fe_B$ are similar. Close examination of the spectra in the $g$ = 6 and $g'$ = 4.3 regions shows that a small increase followed by a decrease is seen in each of the $g$ = 6 and $g'$ = 4.3 signals. This is consistent with an electron reducing one site or the other site in the enzyme population to yield small populations of EPR-visible heme $b_3$ (II) $Fe_B$(III) or heme $b_3$(III) $Fe_B$(II) centres, before full reduction to a homogenous all ferrous state occurs as expected if the reduction potentials of heme $b_3$ and $Fe_B$ are near iso-potential. At pH 8.5 (Fig. 1B), signals which arise from the low spin hemes *b* and *c* again both disappear at +100 mV. The midpoint reduction potential of the $Fe_B$ at pH 8.5 appears to be slightly higher than that of the heme $b_3$; something that is suggested by the slight increase in the intensity of the ferric heme $b_3$ signal in the $g$ = 6 region of the EPR spectra. Overall though, the data shows that the reduction potential of both metals in the active site of NorBC are at a significantly lower reduction potential then that of the electron receiving/storage hemes, heme *c* and heme *b*.

### 3.2. The X-band EPR spectrum of the non-heme iron $Fe_B$

In an attempt to isolate the non-heme iron centre spectroscopically and so obtain direct insight into its redox properties the fact that CO, which is neither paramagnetic nor a substrate for the enzyme, will stabilise the reduced state of heme $b_3$ by forming a His/CO co-ordinated species was exploited [16]. EPR spectra were collected from samples of NorBC poised at a range of potentials under an atmosphere of CO (Fig. 2). As the sample potential was lowered the spectrum becomes dominated by a large axial signal at $g'$ = 4.3 that is characteristic of a high spin, S = 5/2, ferric non heme iron in a low-symmetry environment [17]. Similar spectra have been described in other non heme iron containing proteins, for example transferrin [18] and protocatechuate dioxygenase [19]. The increase in the $g'$ = 4.3 signal, which is attributed to magnetically isolated ferric $Fe_B$, reaches a maximum at +290 mV. These data are consistent with the suggestion that in the presence of CO the effective midpoint reduction potential of heme $b_3$ increases so that it

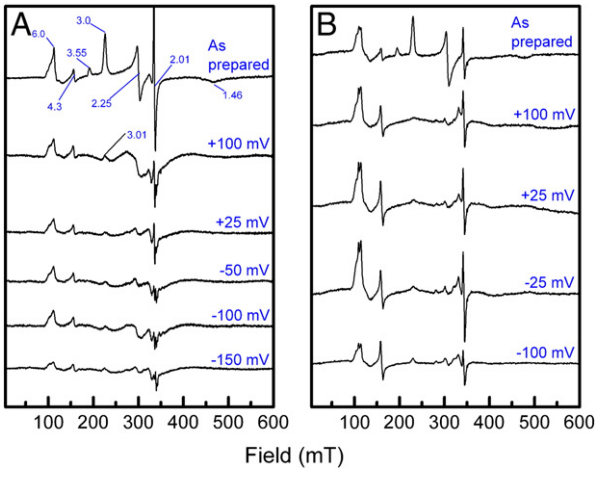


**Fig. 1.** Changes in the X-band EPR spectrum of NorBC as a function of solution potential. Samples were prepared as described in Section 2.1 and EPR spectra subsequently recorded at 10K using the following conditions: microwave frequency of 9.44 GHz, microwave power of 2 mA and a modulation amplitude of 1 mT. Panel A: NorBC (135 μM) in 20 mM BTP, 50 mM NaCl, 0.02% (wt./vol.) DDM, pH 6.0. Panel B: NorBC (135 μM) in 20 mM BTP, 50 mM NaCl, 0.02% (wt./vol.) DDM, pH 8.5.

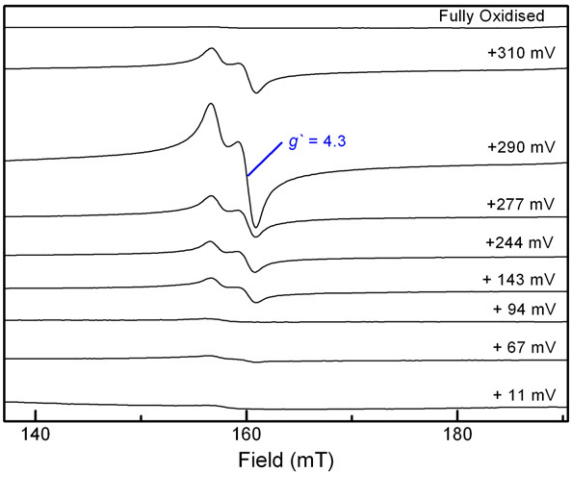


**Fig. 2.** The X-band EPR spectrum of chemically reduced NorBC in the presence of CO. Sample of NorBC (50–60 μM) in 20 mM BTP, 50 mM NaCl, 0.02% (wt./vol.) DDM, pH 6.0. The spectra were recorded at 10K using the following conditions: a microwave frequency of 9.44 GHz, microwave power of 2 mA and a modulation amplitude of 1 mT.

can be reduced independently of $Fe_B$. The consequence of this half reduction of the dinuclear centre is to break the coupling between ferric heme $b_3$ and ferric $Fe_B$ allowing the EPR spectrum of $Fe_B$(III) to be clearly resolved. Reduction to +11 mV results in complete loss of the $Fe_B$(III) signal, suggesting that the presence of CO in the active site also raises the midpoint reduction potential of the $Fe_B$(II/III) couple. The increase in midpoint reduction potential of $Fe_B$ leads to an overlap of the potential ranges in which the heme $b_3$ and $Fe_B$ become reduced. Consequently the signal seen at +290 mV is not representative of 100% ferric $Fe_B$ for two reasons. Firstly at +290 mV the heme $b_3$ is not fully reduced (see Section 3.4); hence, a proportion of the active site remains fully oxidised, coupled and retaining an EPR silent ferric $Fe_B$. Secondly it is conceivable that the midpoint reduction potential of $Fe_B$ is raised sufficiently under a CO atmosphere such that it starts to become reduced before the whole population is released from the coupling with heme $b_3$. Integration of EPR signals at $g' = 4.3$ arising from a high spin, S = 5/2, non heme iron centres is problematic due to the low symmetry of the signals and therefore we are unable to determine the midpoint reduction potential of the non heme $Fe_B$.

### 3.3. Spectroelectrochemical titrations of NorBC

In the light of the EPR data identifying the $Fe_B$(III) signal in heme $b_3$–CO complexed active site and suggesting a low midpoint potential for $Fe_B$ in the CO-free enzyme, a series of visible spectropotentiometric titrations was undertaken in the pH range 6.5–8.5.

Previous analysis of data collected at pH 7.0 described the loss of absorbance at the 595 nm that is associated with complete reduction of the enzyme in terms of three independent $n = 1$ Nernstian curves [11]. The first two phases were interpreted in terms of reduction of $Fe_B$ causing the μ-oxo bridge at the dinuclear centre to break yielding a "*three-electron reduced*" form of the enzyme in which ferric heme $b_3$ exists as a mixture of the His/$H_2O$ and His/$OH^-$ ligated forms [10]. The final phase was attributed to the subsequent reduction of the heme $b_3$.

In the present study, it is instructive to consider the titration carried out at pH 6.5 (Fig. 3). At this pH the 630 nm CT band (Fig. 3C) persists after the loss of the 595 nm band indicating that the heme $b_3$ remains oxidised and has His/$H_2O$ ligation at this point in the titration. Hence the midpoint reduction potential for the heme $b_3$ will be obtained by following the loss of intensity at 630 nm as a function of solution potential. Analysis of this titration gives the midpoint reduction potential for the heme $b_3$ at pH 6.5 to be $E_{m,6.5} = +82$ mV (Fig. 3D). If the oxidised, and presumably high-spin heme $b_3$, that gives rise to the 630 nm band, was the only remaining oxidised centre in the protein then it would be represented in the EPR spectrum at solution potentials >+100 mV by a large signal at $g = \sim 6.0$. This is clearly not the case (Fig. 1) because the ferric heme $b_3$ remains magnetically coupled to the ferric non heme iron and therefore EPR silent.

The midpoint reduction potentials of all three hemes in NorBC are relatively insensitive to changes in pH for the range pH 6.0–8.5 (Fig. 4 and Table 1). However careful examination of the data reveals that in fact it is the oxidation state of the low spin heme *b*, and not $Fe_B$, that influences the ligation state of the ferric high spin heme $b_3$ and hence the accessibility of the active site to substrate. For example, at pH 8.5 and 7.5, the reduction potential of heme *b* can be obtained by fitting the increase in absorbance at 560 nm to a single $n = 1$ Nernstian curve. This gives midpoint reduction potentials for this centre of $E_{m,8.5} = +250$ mV and $E_{m,7.5} = +282$ mV at pH 8.5 and 7.5 respectively. These values are in good agreement with the midpoint reduction potentials obtained from fitting the first phase of the loss of absorbance at 595 nm band at pH 8.5 and 7.5; $E_{m,8.5} = +242$ mV and $E_{m,7.5} = +271$ mV. This suggests that the reduction of the low spin heme *b* can be monitored in two ways, either by the increase in absorbance at 560 nm or by the initial loss of absorbance at 595 nm.

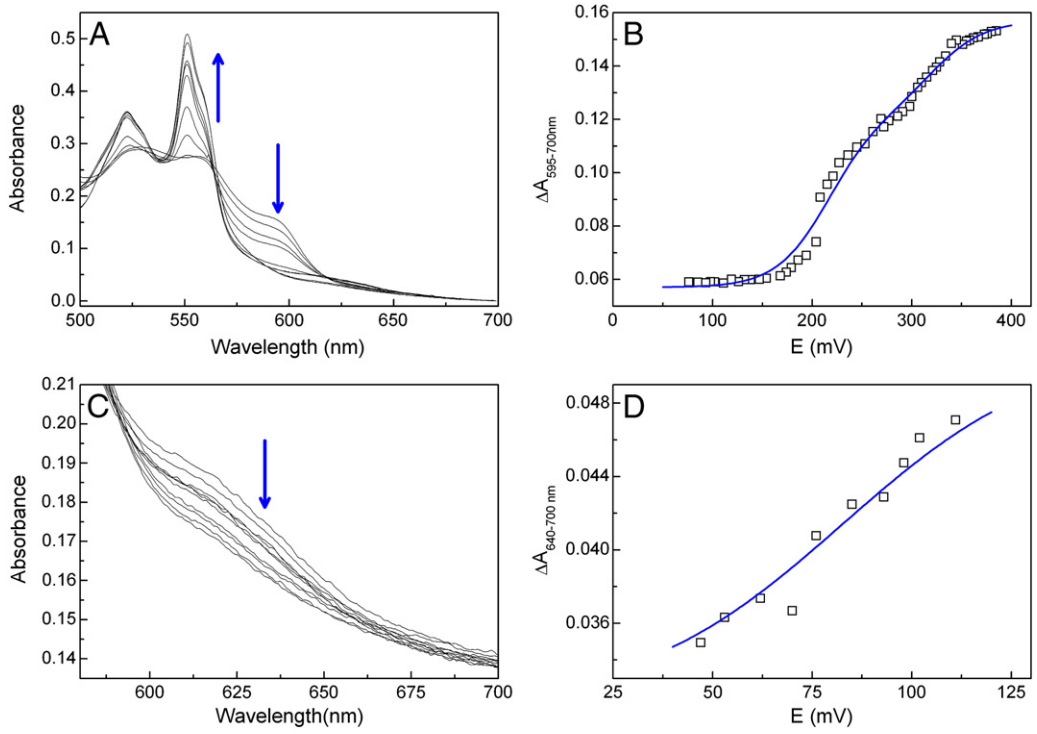


**Fig. 3.** Spectroelectrochemical titration of NorBC. A representative reductive titration of NorBC (10 μM) in 20 mM BTP, 340 mM NaCl, 0.02% (wt./vol.) DDM, pH 6.5 carried out as described in Section 2.4. Panel A: Spectral changes associated with the reduction of NorBC are indicated by arrows. In the interests of clarity only spectra recorded after the addition of every other aliquot of sodium dithionite are shown. Panel B: The loss of absorbance at 595 nm (■) plotted as a function of solution potential. The solid line is a fit to two independent ($n = 1$) Nernstian curves that report the formation of His/$OH^-$ ligated ferric heme $b_3$ ($E_{m,6.5} = +215$ mV) and His/$H_2O$ ligated ferric heme $b_3$ ($E_{m,6.5} = +320$ mV). Panel C: Details of the loss of the 630 nm CT band in response to reduction. Panel D: The loss of absorbance at 630 nm (■) plotted as a function of solution potential. The solid line is a fit to a single $n = 1$ Nernstian curve ($E_{m,6.5} = +82$ mV) that reports the reduction of heme $b_3$.

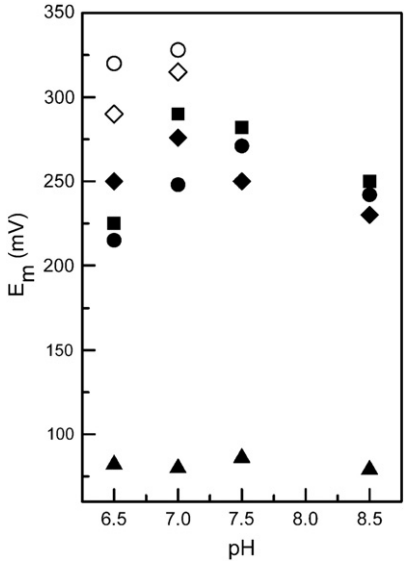


**Fig. 4.** The pH dependence of the observed midpoint reduction potentials of the hemes in NorBC. Midpoint potentials were determined from a series of spectroelectochemical titrations as described in Section 2 and plotted as function of pH as follows. Heme *c* (■) determined from the change in absorbance at 551 nm. Heme *b* first midpoint potential (♦) and second midpoint potential (◊) determined from the change in absorbance at 560 nm. Heme *b* (first midpoint potential) determined from the formation of His/$OH^-$ ligated ferric heme $b_3$ (●). Heme *b* (second midpoint potential) determined from the formation of His/$H_2O$ ligated ferric heme $b_3$ (○). Midpoint reduction potential of heme $b_3$ determined from the change in absorbance at 595 nm (▲).

The initial loss of absorbance at 595 nm associated with the reduction of heme *b* coincides with a shift in the CT band to a longer wavelength which reports the breaking of the μ-oxo bridge and gives information on the subsequent ligation to ferric heme $b_3$. This clearly indicates that reduction of the low spin heme *b* leads to a change in coordination of ferric heme $b_3$ from the μ-oxo bridged form in which the dinuclear centre is closed, to a His/$OH^-$ form in which the dinuclear centre is open and can bind exogenous ligands. It has previously been reported that, below pH 7.5, partial reduction of NorBC results in two heme $b_3$ species, one population with His/$OH^-$ ligation and a second with His/$H_2O$ ligation [10]. This is reflected in the requirement for a two phase fit to the data obtained from monitoring the increase in absorbance at 560 nm associated with the reduction of heme *b* at pH 6.5. The high potential phase of reduction is concomitant with a change of ligation from a μ-oxo bridged active site to His/$H_2O$ ligation of the heme $b_3$, $E_{m,6.5} = +290$ mV. The low potential phase pertains to the reduction of the heme *b* when the μ-oxo bridge breaks to form a His/$OH^-$ ligated heme $b_3$, $E_{m,6.5} = +225$ mV. These potentials are very close to those obtained from the first two phases associated with the loss of the 595 nm band at pH 6.5 which give midpoint reduction potentials for the reduction of heme *b* and the associated ligation change at the heme $b_3$ to His/OH of $E_{m,6.5} = +215$ mV and to His/$H_2O$ of $E_{m,6.5} = +320$ mV.

Taken together these data strongly suggest that the reduction of the low spin heme *b* causes the proximal histidine (His-334) to ligate the active site heme $b_3$ and cause the μ-oxo bridge to break. This proposal is broadly consistent with the recently published structure of the *P. aeruginosa* enzyme which is in the half-reduced state due to the very rapid reduction of the high potential hemes, heme *c* and heme *b*, in the X-ray beam [5]. It is also perhaps not too surprising since the structure of NorB also shows that the axial ligand to heme *b* (His-336) and the proximal ligand to heme $b_3$ (His-334) are on opposite faces of transmembrane helix 10 [5]. The intervening residue is a glycine (Gly-335) which might suggest some conformational flexibility in this region of the helix.

### 3.4. The effect of CO on the midpoint reduction potential of heme $b_3$

Spectroelectrochemical titrations of NorBC collected under an atmosphere of CO revealed that as the potential is reduced signals in the α and β regions increase in intensity as the low spin hemes *b* and *c* become reduced (Fig. 5A). The changes in absorbance at 551 nm and 560 nm can be plotted against potential and fitted to $n = 1$ Nernstian curves (Fig. 5B and C) to give midpoint reduction potentials for the low spin hemes *b* and *c* under a CO atmosphere of +297 mV and +273 mV respectively. These values are in good agreement with those seen for these centres without CO present and using a chemical reductant, suggesting that neither the manner of reduction nor presence of a substrate analogue has a significant effect on their reduction potential.

Simultaneously, intensity is completely lost from the 595 nm CT band arising from the oxidised, μ-oxo bridged, heme $b_3$ as this centre also becomes reduced. This is in contrast to the situation during titrations without CO present where the CT band shifts to longer wavelengths on the reduction of the low spin hemes before the heme $b_3$ becomes reduced at lower potential (Fig. 3A). Consequently, the change in absorbance at 595 nm can be fitted to a single $n = 1$ Nernstian curve giving a midpoint reduction potential for the heme $b_3$ of +303 mV under a CO atmosphere (Fig. 5D). This shift to higher potential of over 200 mV in response to the presence of CO is comparable to that reported for the active site heme $o_3$ in a form of the canonical HCuO cytochrome $bo_3$ oxidase that lacks $Cu_B$ in its dinuclear centre [20] In the case of the active site of NorBC the increase in the reduction potential of the catalytic heme elicited by the presence of CO raises it to the region in which the electron transfer hemes become reduced.

## 4. Conclusions

We have shown that the redox centres at the active site of NorBC are at isopotential with midpoint reduction potentials of $E_m \approx +80$ mV. Given that these values lie below those of hemes *b* and *c* at *ca.* +300 mV it would appear that heme *c* and heme *b* act as an electron receiving/storage module and that in the absence of substrate the active site does not become substantially reduced on reduction of both the low spin hemes *b* and *c*. However, reduction of the low spin heme *b* leads to breaking of the μ-oxo bridge in the

**Table 1**
Effect of pH and CO exposure on the midpoint reduction potentials of the hemes in NorBC.

| pH | Em (mV) | | | | | |
|---|---|---|---|---|---|---|
| | Heme *c* (551 nm) | Heme *b* First midpoint potential (560 nm) | Heme *b* Second midpoint potential (560 nm) | Heme *b* First midpoint potential (595 nm) heme $b_3$ forms His/$OH^-$ | Heme *b* Second midpoint potential (560 nm) heme $b_3$ forms His/$H_2O$ | Heme $b_3$ |
| 8.5 | 230 | 250 | | 242 | | [a]82 |
| 7.5 | 250 | 282 | | 271 | | [a]80 |
| 7.0 | 276 | 290 | 315 | 248 | 328 | [a]86 |
| 6.5 | 250 | 225 | 290 | 215 | 320 | [b]79 |
| 6.0 (under CO atmosphere) | 273 | 297 | | | | [a]303 |

[a] Determined at 595 nm.
[b] Determined at 640 nm.

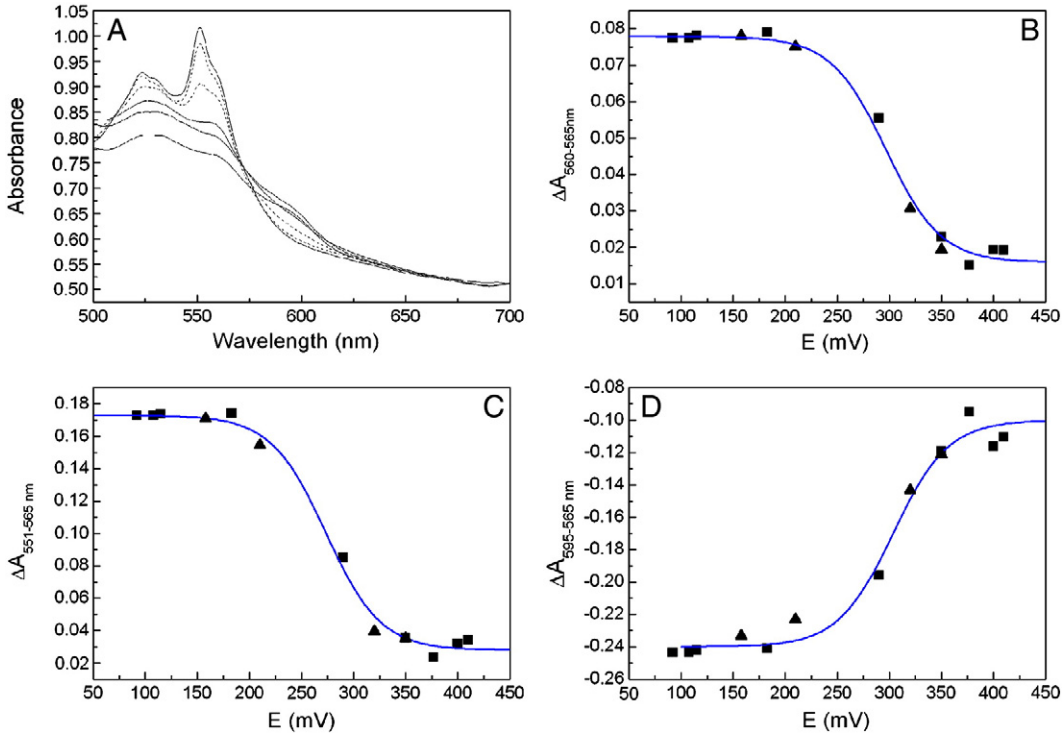


**Fig. 5.** The effect of CO on the midpoint reduction potential of heme $b_3$. Spectral changes in NorBC (20 μM) in 20 mM BTP, 100 mM NaCl, 0.02% (wt./vol.) DDM, pH 6.0 under an atmosphere of CO were recorded as a function of solution potential as described in Section 2.6. Panel A: Representative spectra recorded during reductive (solid line) and oxidative (dashed line) titrations. Panel B: Changes in absorbance at 560 nm associated with oxidation/reduction of heme *b* plotted as function of solution potential. The data points were recorded either during reductive (■) or oxidative (▲) titrations and the solid line is a fit to a $n=1$ Nernstian curve ($E_{m,6.0}=+297$ mV). Panel C: Changes in absorbance at 551 nm associated with oxidation/reduction of heme *c* plotted as function of solution potential. The data points were recorded either during reductive (■) or oxidative (▲) titrations and the solid line is a fit to a $n=1$ Nernstian curve ($E_{m,6.0}=+273$ mV). Panel D: Changes in absorbance at 595 nm associated with oxidation/reduction of heme $b_3$ plotted as function of solution potential. The data points were recorded either during reductive (■) or oxidative (▲) titrations and the solid line is a fit to a $n=1$ Nernstian curve ($E_{m,6.0}=+303$ mV).

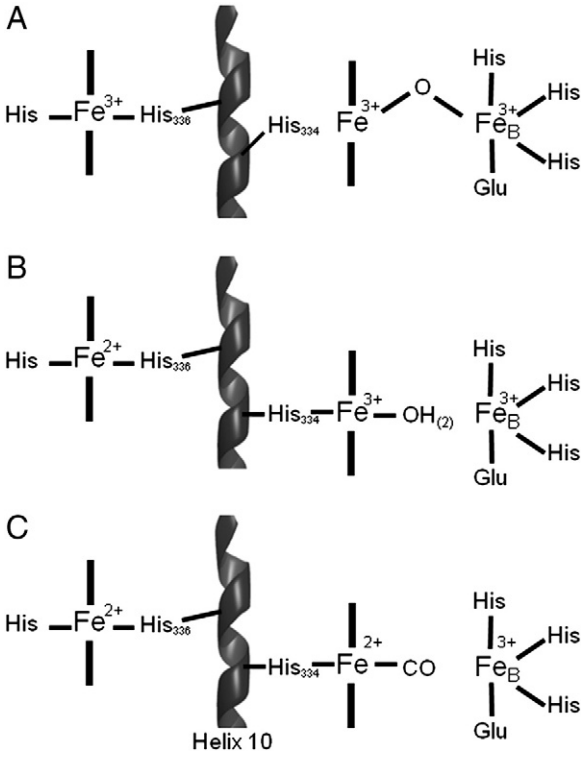


**Fig. 6.** Schematic diagram showing a possible mechanism reductive activation and electron transfer in NorBC. A shows the μ-oxo bridged dinuclear centre in the as isolated protein. B shows the opening of the active site and binding of the proximal histidine to heme $b_3$ upon reduction of the low spin heme *b*. C shows the CO bound species after electron transfer to the active site and re-reduction of heme *b* by heme *c*.

oxidised dinuclear centre and in turn leads to the opening of the active site to allow binding of substrate molecules (Fig. 6B). In the presence of CO, a substrate analogue, the reduction potential of the heme $b_3$ is raised sufficiently to initiate proton-coupled electron transfer to the active site. It is conceivable that binding of the natural substrate, NO, to heme $b_3$ would elicit the same effect. (Fig. 6C). Thus, we postulate that reduction of the electron transfer hemes leads to an opening of the active site which allows access to substrate which in turn raises the reduction potential of the active site heme $b_3$ such that electrons are only delivered to the active site when substrate is present and able to form a ferrous-NO heme $b_3$ species.

The participation of such an intermediate would be consistent with the results obtained in a recent study of the reaction of fully reduced NorBC with NO using the flow–flash approach [21]. In this experiment the four-electron reduced enzyme is able to complete two turnovers; the first turnover using the electrons in the active site and the second using the electrons stored by heme *c* and heme *b*. Consequently the second turnover must involve electron transfer to the active site in the presence of substrate. The rate of electron transfer to the active site is clearly dependent on the concentration of NO, with the rate of internal electron transfer increasing as the NO concentration is lowered [21]. This is consistent with an earlier report of substrate inhibition of NorBC [22] and reports of the steady state concentration of NO in cultures of actively denitrifying *P. denitrificans* being as low as 20 nM [23] which is still considerably higher than the $K_D$ ($1\times10^{-12}$ M) for NO binding to the ferrous heme *b* in myoglobin [24].

Previous consideration of the mechanism of NO reduction by the bacterial NOR has focussed on whether one or both metal centres in the active site bind substrate molecules. In the so-called *cis* mechanism it is envisaged that both NO molecules bind to $Fe_B$ [25], while in the *trans* mechanism one NO molecule would bind to $Fe_B$ and the other to heme

$b_3$ [9,26]. Until recently less emphasis has been given to the way in which the enzyme orchestrates the arrival of its co-substrates, 2NO, two electrons and two protons, at the active site to minimise the opportunity for unwanted reactions. The results presented here seem to argue that initial binding of the first NO molecule would be to the oxidised heme $b_3$, something that would exclude the *cis* mechanism and be consistent with computational studies [27], which suggest that the role of $Fe_B$ is to stabilise a hyponitrite intermediate. Further experiments will be required in order to determine if the second molecule of NO binds to $Fe_B$ or if reacts directly with the NO bound to the heme $b_3$ to form the hyponitrite intermediate which then decomposes to form the product, $N_2O$ and possibly reform the μ-oxo bridge.

## Acknowledgments

The work reported here was supported by the UK Biotechnology and Biological Sciences Research Council (BBC0077191). We would like to thank Dr Shirley Fairhurst, John Innes centre, Norwich for the help in collecting the EPR spectra and Verity Lyall for her technical assistance.

## References

[1] N.J. Watmough, S.J. Field, R.J. Hughes, D.J. Richardson, The bacterial respiratory nitric oxide reductase, Biochem. Soc. Trans. 37 (2009) 392–399.
[2] W.G. Zumft, Nitric oxide reductases of prokaryotes with emphasis on the respiratory, heme–copper oxidase type, J. Inorg. Biochem. 99 (2005) 194–215.
[3] D.J. Richardson, N.J. Watmough, Inorganic nitrogen metabolism in bacteria, Curr. Opin. Chem. Biol. 3 (1999) 207–219.
[4] D. Richardson, H. Felgate, N. Watmough, A. Thomson, E. Baggs, Mitigating release of the potent greenhouse gas N(2)O from the nitrogen cycle—could enzymic regulation hold the key? Trends Biotechnol. 27 (2009) 388–397.
[5] T. Hino, Y. Matsumoto, S. Nagano, H. Sugimoto, Y. Fukumori, T. Murata, S. Iwata, Y. Shiro, Structural basis of biological N2O generation by bacterial nitric oxide reductase, Science 330 (2010) 1666–1670.
[6] F.H. Thorndycroft, G. Butland, D.J. Richardson, N.J. Watmough, A new assay for nitric oxide reductase reveals two conserved glutamate residues form the entrance to a proton-conducting channel in the bacterial enzyme, Biochem. J. 401 (2007) 111–119.
[7] J. Hemp, H. Han, J.H. Roh, S. Kaplan, T.J. Martinez, R.B. Gennis, Comparative genomics and site-directed mutagenesis support the existence of only one input channel for protons in the C-family ($cbb_3$ oxidase) of heme–copper oxygen reductases, Biochemistry 46 (2007) 9963–9972.
[8] M.R. Cheesman, W.G. Zumft, A.J. Thomson, The MCD and EPR of the heme centers of nitric oxide reductase from *Pseudomonas stutzeri*: evidence that the enzyme is structurally related to the heme–copper oxidases, Biochemistry 37 (1998) 3994–4000.
[9] P. Moënne-Loccoz, S. de Vries, Structural characterization of the catalytic high-spin heme *b* of nitric oxide reductase: a resonance Raman study, J. Am. Chem. Soc. 120 (1998) 5147–5152.
[10] K.L. Grönberg, N.J. Watmough, A.J. Thomson, D.J. Richardson, S.J. Field, Redox-dependent open and closed forms of the active site of the bacterial respiratory nitric oxide reductase revealed by cyanide binding studies, J. Biol. Chem. 279 (2004) 17120–17125.
[11] S.J. Field, L. Prior, M.D. Roldan, M.R. Cheesman, A.J. Thomson, S. Spiro, J.N. Butt, N.J. Watmough, D.J. Richardson, Spectral properties of bacterial nitric-oxide reductase: resolution of pH-dependent forms of the active site heme $b_3$, J. Biol. Chem. 277 (2002) 20146–20150.
[12] K.L.C. Grönberg, M.D. Roldán, L. Prior, G. Butland, M.R. Cheesman, D.J. Richardson, S. Spiro, A.J. Thomson, N.J. Watmough, A low-redox potential heme in the dinuclear center of bacterial nitric oxide reductase: implications for the evolution of energy-conserving heme–copper oxidases, Biochemistry 38 (1999) 13780–13786.
[13] S.J. Field, F.H. Thorndycroft, A.D. Matorin, D.J. Richardson, N.J. Watmough, The respiratory nitric oxide reductase (NorBC) from *Paracoccus denitrificans*, Methods Enzymol. 437 (2008) 79–101.
[14] K.A. Vincent, G.J. Tilley, N.C. Quammie, I. Streeter, B.K. Burgess, M.R. Cheesman, F.A. Armstrong, Instantaneous, stoichiometric generation of powerfully reducing states of protein active sites using Eu(II) and polyaminocarboxylate ligands, Chem. Comm. (2003) 2590–2591.
[15] P.L. Dutton, Redox potentiometry: determination of midpoint potentials of oxidation–reduction components of biological electron-transfer systems, Methods Enzymol. 54 (1978) 411–435.
[16] J.H. Hendriks, L. Prior, A.R. Baker, A.J. Thomson, M. Saraste, N.J. Watmough, Reaction of carbon monoxide with the reduced active site of bacterial nitric oxide reductase, Biochemistry 40 (2001) 13361–13369.
[17] E.I. Solomon, T.C. Brunold, M.I. Davis, J.N. Kemsley, S.K. Lee, N. Lehnert, F. Neese, A.J. Skulan, Y.S. Yang, J. Zhou, Geometric and electronic structure/function correlations in non-heme iron enzymes, Chem. Rev. 100 (2000) 235–350.
[18] R. Aasa, B.G. Malmstroem, P. Saltman, The specific binding of iron(III) and copper (II) to transferrin and conalbumin, Biochim. Biophys. Acta 75 (1963) 203–222.
[19] H. Fujisawa, M. Uyeda, Y. Kojima, M. Nozaki, O. Hayaishi, Protocatechuate 3,4-dioxygenase. II. Electron spin resonance and spectral studies on interaction of substrates and enzyme, J. Biol. Chem. 247 (1972) 4414–4421.
[20] J.C. Salerno, B. Bolgiano, R.K. Poole, R.B. Gennis, W.J. Ingledew, Heme–copper and heme–heme interactions in the cytochrome bo-containing quinol oxidase of *Escherichia coli*, J. Biol. Chem. 265 (1990) 4364–4368.
[21] P. Lachmann, Y. Huang, J. Reimann, U. Flock, P. Ädelroth, Substrate control of internal electron transfer in bacterial nitric-oxide reductase, J. Biol. Chem. 285 (2010) 25531–25537.
[22] P. Girsch, S. de Vries, Purification and initial kinetic and spectroscopic characterization of NO reductase from *Paracoccus denitrificans*, Biochim. Biophys. Acta 1318 (1997) 202–216.
[23] L. Molstad, P. Dörsch, L.R. Bakken, Robotized incubation system for monitoring gases (O2, NO, N2O N2) in denitrifying cultures, J. Microbiol. Meth. 71 (2007) 202–211.
[24] E.A. Brucker, J.S. Olson, M. Ikeda-Saito, G.N.J. Phillips, Nitric oxide myoglobin: crystal structure and analysis of ligand geometry, Proteins 30 (1998) 352–356.
[25] N.J. Watmough, M.R. Cheesman, C.S. Butler, R.H. Little, C. Greenwood, A.J. Thomson, The dinuclear center of cytochrome $bo_3$ from *Escherichia coli*, J. Bioenerg. Biomemb. 30 (1998) 55–62.
[26] I.M. Wasser, S. de Vries, P. Moënne-Loccoz, I. Schroder, K.D. Karlin, Nitric oxide in biological denitrification: Fe/Cu metalloenzyme and metal complex NO(x) redox chemistry, Chem. Rev. 102 (2002) 1201–1234.
[27] L.M. Blomberg, M.R. Blomberg, P.E. Siegbahn, Reduction of nitric oxide in bacterial nitric oxide reductase—a theoretical model study, Biochim. Biophys. Acta 1757 (2006) 240–252.